Bioconjugate Chemistry

Article

Imaging and Quantitative Detection of Lipid Droplets by Yellow Fluorescent Probes in Liver Sections of Plasmodium Infected Mice and Third Stage Human Cervical Cancer Tissues

Ashutosh Sharma, Ajay Kumar Jha, shachi mishra, Ankita Jain, Bhavana S Chauhan, Manoj Kathuria, Kundan Singh Rawat, Neeraj Mohan Gupta, Renu Tripathi, Kalyan Mitra, Monika Sachdev, Madan L Bhatt, and Atul Goel

Bioconjugate Chem., **Just Accepted Manuscript** • DOI: 10.1021/acs.bioconjchem.8b00552 • Publication Date (Web): 24 Sep 2018

Just Accepted

ACS Publications

is published by the American Chemical Society. 1155 Sixteenth Street N.W., Washington, DC 20036

Imaging and Quantitative Detection of Lipid Droplets by Yellow Fluorescent Probes in Liver Sections of *Plasmodium* Infected Mice and Third Stage Human Cervical Cancer Tissues

Ashutosh Sharma,[a] Ajay K. Jha,[a] Shachi Mishra,[a] Ankita Jain,[b] Bhavana S. Chauhan,[c] Manoj Kathuria,[d] Kundan S. Rawat,[a,f] Neeraj M. Gupta,[a] Renu Tripathi,[c] Kalyan Mitra,[d] Monika Sachdev,[b] Madan L.B. Bhatt,[e] Atul Goel*[,a,f]

[a] Fluorescent Chemistry Lab, Medicinal and Process Chemistry Division, CSIR-Central Drug Research Institute, Lucknow 226031, India

[b] Endocrinology Division, CSIR-Central Drug Research Institute, Lucknow 226031 (India).

[c] Parasitology Division, CSIR-Central Drug Research Institute, Lucknow 226031 (India).

[d] Electron Microscopy Unit, CSIR-Central Drug Research Institute, Lucknow 226031 (India).

[e] Department of Radiotherapy, King George's Medical University , Lucknow, 226003 (India).

[f] Academy of Scientific and Innovative Research, Ghaziabad 201 002 (India)

E-mail: atul_goel@cdri.res.in

KEYWORDS: Fluorescent probes • Lipid droplets • Cervical cancer • Quantitative detection • Tissue Imaging

ABSTRACT: The diagnosis and prognosis of the disease associated with lipid irregularity is an area of extreme significance. In this direction, fluoranthene based yellow fluorescent probes (**FLUN-550**, **FLUN-552**, **FLUN-547**) were designed and synthesized by conjugating ethanolamine head group of the phospholipid phosphatidyl-ethanolamine present in biological membranes. Owing to unique photophysical properties and aqueous compatibility, these probes were successfully employed for staining lipid droplets (LDs) in pre-adipocytes and *Leishmania donovani* promastigotes. Furthermore, using the fluorescent probes **FLUN-**

550 and **FLUN-552** we successfully imaged and quantitatively detected the excess accumulation of lipids in liver section of Plasmodium yoelii MDR infected mouse (3- to 4-fold) and the tissue sections of third stage human cervical cancer patients (1.5- to 2-fold) compared to normal tissues. To the best of our knowledge, this is the first report of yellow fluorescent probes for imaging and quantitative detection of LDs in human cervical cancer tissues. These new yellow fluorescent lipid probes (**FLUN-550** and **FLUN-552**) showed great potential for early diagnosis of cervical cancer patients.

▪ INTRODUCTION

Lipid droplets (LDs) are dynamic organelles in the cells which are considered as a place for energy storage and are significantly involved in the lipid metabolic events.[1,2] The abnormalities in the function of LDs have significant effects on the pathogenesis of diabetes, obesity and cardiovascular diseases. Liver is the main organ of the human body that controls the lipid metabolism.[3,4] Literature reports revealed that LDs play a key role in the production and assembly of hepatitis C virus, a causative agent of chronic liver diseases.[2,5] The methods generally used to access the LDs level are ultrasound and computerized tomography scanning but these analyses are not precise and can detect only ~25% of the fat content in the liver.[6] Transhepatic biopsy is the only method to diagnose the early stage liver disease with high sensitivity. Hence, the direct monitoring and localizing the accumulation of abnormal level of LDs in the liver tissue is a thrust area of research. Further cancerous tissues have been recognized to exhibit specific alterations in their metabolic activity which is thought to facilitate the rapid proliferation of transformed cells. Earlier reports suggest increased rate of lipid biosynthesis in cancerous tissues that are comparable to liver tissues, which have a high rate of fatty acid biosynthesis.[7,8] Despite of the growing evidence demonstrating deregulated lipid biosynthesis as features of cancer, the mechanism of these metabolic alterations in the development of the disease is not fully understood. Therefore, diagnostic tools for detection,

imaging and quantification of lipid droplets in infected/cancerous and normal tissues are highly desirable for understanding and unravelling the mysteries associated with lipid structure, biosynthesis and metabolism.[9]

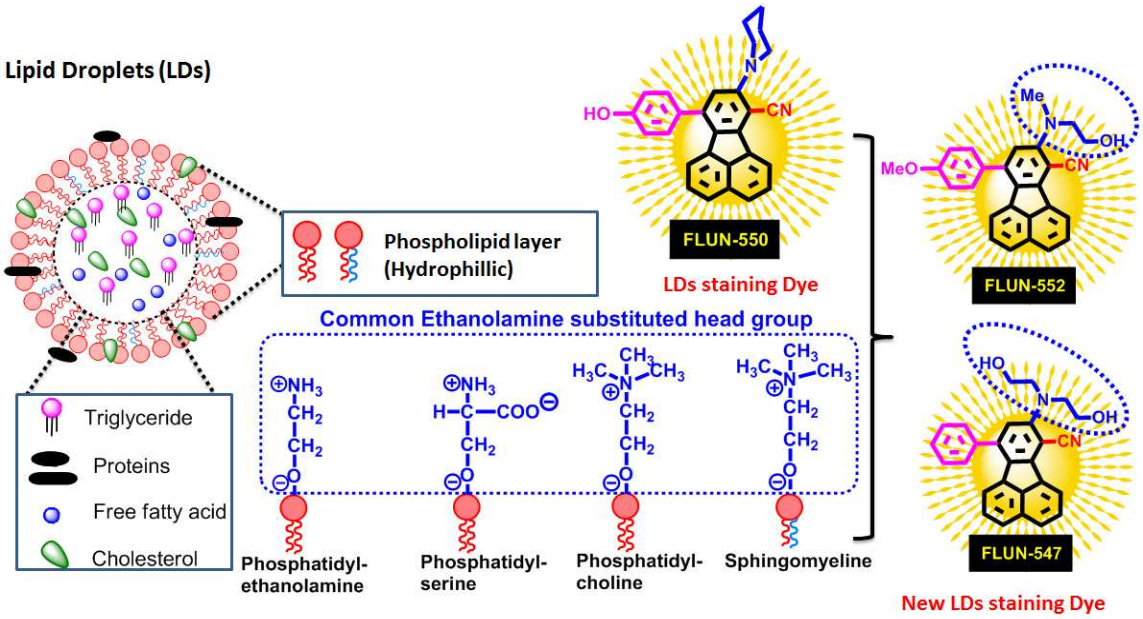

Figure 1. Designing strategy of newly synthesized Fluoranthene based LDs staining dyes.

The Oil Red O (ORO) (non-fluorescent dye), Nile Red and BODIPY dyes are commonly used commercial dyes to measure LDs in cells and tissues.[10-16] However, these dyes have some limitations, like for ORO staining fixation is required thus preventing its use in live cells; solubility issues and stability problems on prolonged usage further limit its scope. LDs probe Nile Red also stains other hydrophobic structures in the cell resulting in low LD selectivity and has small Stokes shifts and thus induce nonradiative energy transfers and show interference from scattered light ultimately leading to unfavorable signal-to-noise ratio and background artifacts.[17-19] In recent past, several new fluorescent probes[20-36] such as monodansylpentane, AFN, NPBDP, LipidTOX red, SF44, FAS, FLUN-550, TPA-BI and LD540 for staining LDs in live and fixed cells have been developed, however they have not been explored for quantitative detection of LDs in infected/cancerous specimens.

LDs are primarily composed of a cluster of lipid esters (triacylglycerol, steryl esters) covered with a phospholipid monolayer.[9] The phospholipids that are predominantly found in the plasma membrane of mammalian cells are mainly *Phosphatidylcholine, Phosphatidylethanolamine, Phosphatidyl-serine,* and *Sphingomyelin* (Figure 1). In this manuscript, we designed and synthesized fluoranthene based fluorescent dyes by anchoring ethanolamine head group of the phospholipid phosphatidyl-ethanolamine for specific staining of LDs in pre-adipocyte, *L. donovani*, plasmodium infected liver sections and the tissues of third stage of human cervical cancer patients. Recently we have discovered[37] a new fluorescent probe **FLUN-550** with good biocomapatibility and cellular uptake for selective staining and quantification of LDs in pre-adipocyte, *L. donovani* and *C. elegans.*[24] Taking into account the ampiphillic nature and composition of LDs, new derivatives of fluoranthene (**FLUN**) with mono- or di-ethanolamine moieties were designed and synthesized. The adopted synthetic strategy is represented in the Scheme 1.

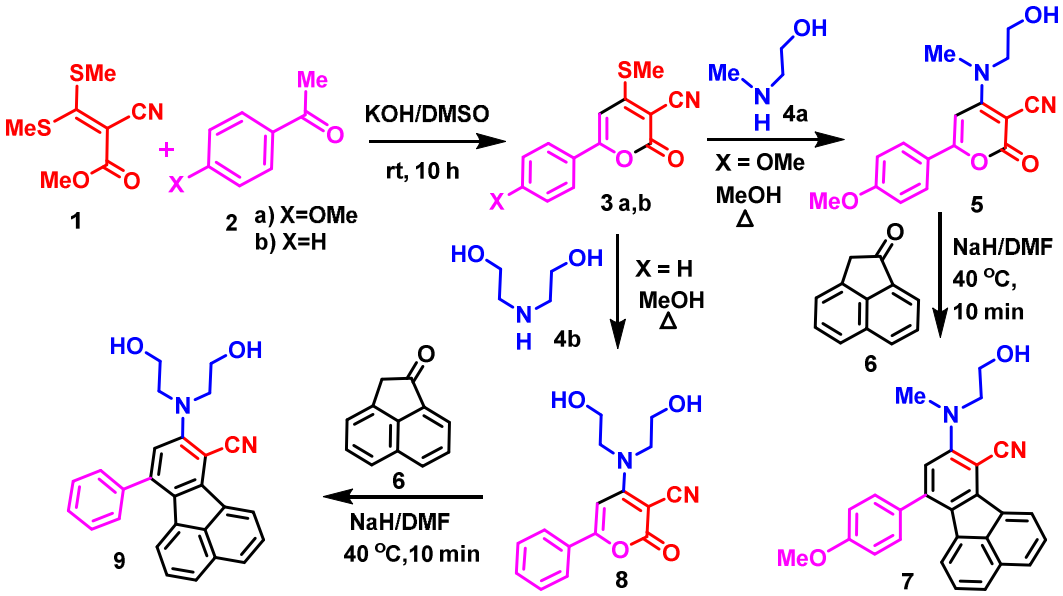

Scheme 1. Synthesis of **FLUN** derivatives with methyl-ethanolamine and diethanolamine as a donor group.

RESULTS AND DISCUSSION

Molecular design and synthesis

The aryl ketones **2a,b** on reaction with ketene dithioacetal **1** in presence of base led to the formation of 6-aryl-4-(methylthio)-2-oxo-2*H*-pyran-3-carbonitriles[24] (**3a,b**) which were substituted with *N*-methylethanolamine (**4a**) and bis-2-hydroxyethylamine (**4b**) to give 4-((2-hydroxyethyl)(methyl)amino)-6-(4-methoxyphenyl)-2-oxo-2*H*-pyran-3-carbonitrile (**5**) and 4-(bis(2-hydroxyethyl)amino)-2-oxo-6-phenyl-2*H*-pyran-3-carbonitrile (**8**) respectively.[38] The compounds **5** and **8** on reaction with acenaphthylen-1(2*H*)-one (**6**) in the presence of a base resulted in the formation of 8-((2-hydroxyethyl)(methyl)amino)-10-(4-methoxyphenyl)-fluoranthene-7-carbonitrile (**7**) and 8-(bis(2-hydroxyethyl)-amino)-10-phenyl-fluoranthene-7-carbonitrile (**9**) respectively in good yields.

Photophysical studies of synthesized fluorescent probes

The photophysical properties of the synthesized **FLUN** derivatives **7** and **9** in PBS buffer (pH 7.2) showed absorption maxima at 342 and 335 nm ($\pi \rightarrow \pi^*$) along with low intensity charge transfer band at 445 and 440 nm ($n \rightarrow \pi^*$) respectively. Photoluminescence (PL) spectra of **7** and **9** showed maxima at 552 and 547 nm respectively with good quantum yield in DMSO and PBS (Figure 2, Table S1). These **FLUN** derivative **7** (**FLUN-552**) and **9** (**FLUN-547**) exhibited high Stokes shifts of 210 nm and 212 nm respectively in buffer solution. The solvatochromic study in solvents of varying polarity showed the intramolecular charge transfer characteristics of these fluorescent probes (Figure S1). The fluorescent probes **FLUN-552** and **FLUN-547** were found to be highly emissive in non-polar solvents like cyclohexane and toluene suggesting their potential application in hydrophobic cellular environment like lipids (Figure S1 and S2). As in biochemical systems, pH plays an important role in conducting different cellular events or processes. The fluorescence

properties of the **FLUN** derivatives at different pH values (~1–12) were investigated. These probes were found to be stable at pH range ~6–8, but slight variation in the fluorescence intensity was observed beyond these ranges (Figure S3).

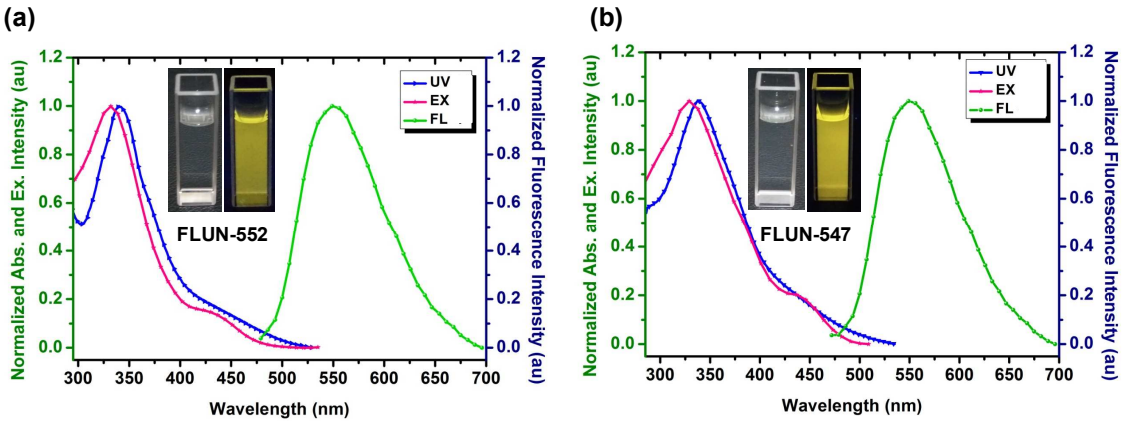

Figure 2. Excitation and fluorescence spectra of **FLUN-552** and **FLUN-547** in PBS buffer (pH 7.2, ~10^{-5} M). Image of compounds in normal and UV light

DFT study of FLUNs

To gain insight into the electronic properties, time-dependent density functional theory (TD-DFT) calculations for FLUN-552 and FLUN-547 were performed using B3LYP/6-311++G (d,p) method employing Gaussian 09 package. Molecular orbitals in the ground and excited state for **FLUN- 552** and **FLUN-547** are represented in Supporting information (Figure S4 and Figure S5). TD-DFT calculations of **FLUN-552** indicated strong transition at 447 nm with an oscillator strength of $f = 0.0513$ corresponding to HOMO → LUMO, while **FLUN-547** showed strong transition at 438 nm with an oscillator strength of $f = 0.0464$ corresponding to HOMO→ LUMO. The transition band at higher wavelength may be attributed to an intramolecular charge transfer (ICT) which was observed from the charge transfer from HOMO (dispersed on the hydroxyl amine donor and central aromatic ring) to LUMO (localised on the core fluoranthene scaffold). The change in planarity of FLUN

derivatives due to the aryl and alkylamino substituents shifts the electron density towards the fluoranthene ring (LUMO). The band gap, transition energies, oscillator strengths, and assignments for the most relevant excited states of **FLUN-552** and **FLUN-547** are presented in Table S2.

LDs staining in 3T3-L1 pre-adipocytes and *L. donovani*

Considering the lipid droplets staining property of **FLUN-550**, we investigated the staining pattern of newly synthesized **FLUN-552** and **FLUN-547** in 3T3-L1 pre-adipocytes. Interestingly, confocal fluorescence microscopy imaging studies revealed that **FLUN-552** and **FLUN-547** selectively stained the lipid droplets (LDs) of pre-adipocytes at 100 nM concentration (Figure S6). To confirm LDs staining, dual staining experiments were performed with Nile Red in 3T3-L1 pre-adipocytes, which revealed specific localization in distinct cytoplasmic lipid droplets present in these cells (Figure 3) and clearly showed co-localization of the Nile Red with **FLUN-552** (Figure 3, A-D) and **FLUN-547** (Figure 3, E-H) within LDs. These **FLUN** derivatives **FLUN-552** and **FLUN-547** at 100 nM concentration showed bright fluorescence staining without background noise. This shows the advantage of **FLUN** dyes with a high Stokes shift that can be used at nanomolar concentrations without fluorescence bleeding. Cell viability experiments revealed that FLUN-550, FLUN-552 and FLUN-547 dyes have no significant cytotoxicity in preadipocytes 3T3-L1 up to the concentration of 2 μM for 48 hours and 72 hours (Figure S7). Approximately 93-94% 3T3-L1 cells were observed to be viable even at 2 μM of FLUN derivatives for up to 72 hours (see Figure S7 in supporting information).

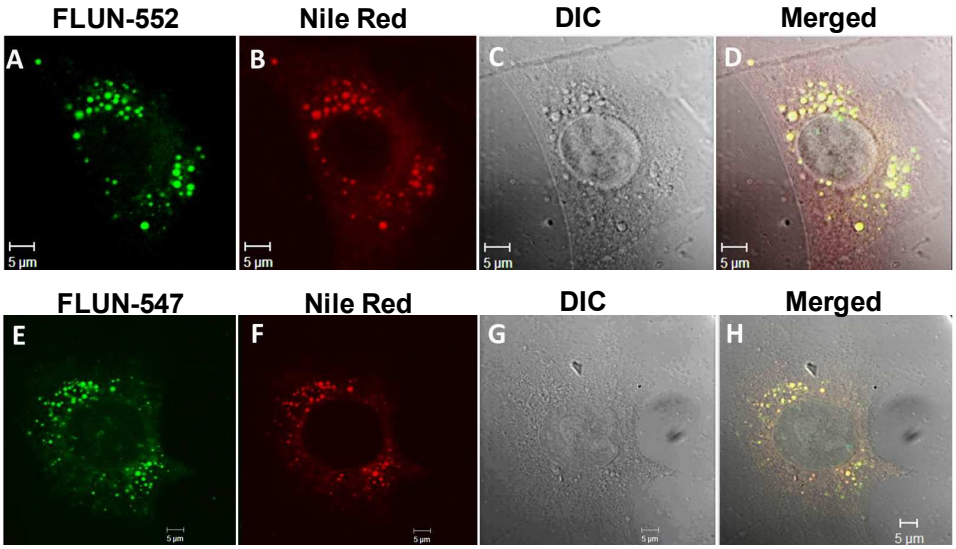

Figure 3. Confocal fluorescence image of 3T3-L1 Pre-adipocytes stained with 100 nM of **FLUN-552** and **FLUN-547** with Nile Red (300 nM) for 30 min. at 37°C. For **FLUN-552** and **FLUN-547**, λ_{ex}= 405 nm, λ_{em} =505 nm-570 nm; Bar indicates 5 µm.

After selective staining of cytoplasmic LDs by FLUNs in adipocytes, we further explored their potential for imaging LDs in live *Leishmania donovani* parasites, the causative protozoan for the disease Visceral Leishmaniasis (KALA-AZAR).[39] Studies have shown that lysophospholipid analogues (LPAs) like Edelfosine, Ilmofosine and Miltefosine (FDA approved antileishmanial drugs) interact with various sub-cellular structures and enzymes especially those associated with cellular membranes thus interfering with lipid metabolism of *Leishmania donovani* promastigotes.[40,41] In this direction *L. donovani* promastigotes were incubated with 100 nM of **FLUN-552** and **FLUN-547** for 2h at physiological conditions. Confocal microscopic observations of *L. donovani* stained with **FLUN-552** and **FLUN-547** revealed localized fluorescence within specific spherical compartments of the cells (Figure S8). Similar localization in *L. donovani* promastigotes was observed with the fluorescent LD stain, Nile Red. Furthermore, dual staining of *L. donovani* promastigotes with Nile Red and **FLUN** derivatives confirmed the specific localization in distinct LDs with no labelling in

nucleus and other organelles present in these cells. Thus, it is evident that **FLUN-552** and **FLUN-547** fluoresces selectively in the LDs region of the parasite with high brightness without background noise (Figure 4). The toxicity assessment data showed that **FLUN** derivatives are non-toxic to *L. donovani* up to 1μM concentration and there was no morphological deformity in the promastigotes during the experimental conditions.

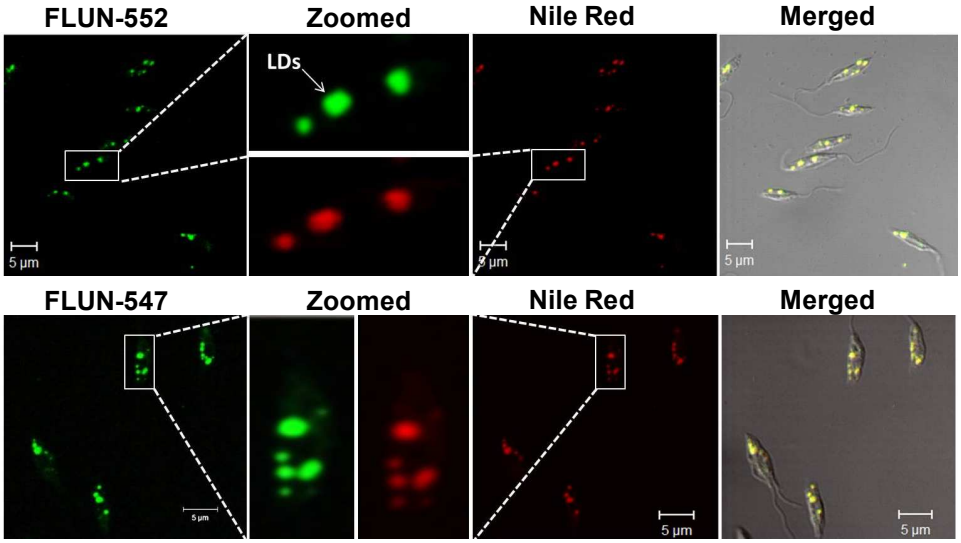

Figure 4. Confocal fluorescence image of *L. donovani* promastigotes stained with 100 nM of **FLUN-552** and **FLUN-547** with Nile Red. Bar indicates 5 μm.

LDs staining in healthy and infected liver tissue sections

The understanding of lipid accumulation in the pathogenesis of malaria is of utmost importance. The studies with rodent malaria parasite *Plasmodium yoelii* nigeriensis MDR have shown that at high parasitaemia, this parasite induces lipid infiltration in liver of showed scanty deposition of lipid droplets [42,43]. After deposition, lipids undergo peroxidation infected mice. The lipid deposition start appearing early in infection but become most pronounced with the increasing level of parasitaemia (30-45%) while liver of healthy mice and ultimately lead to hepatic tissue damage.

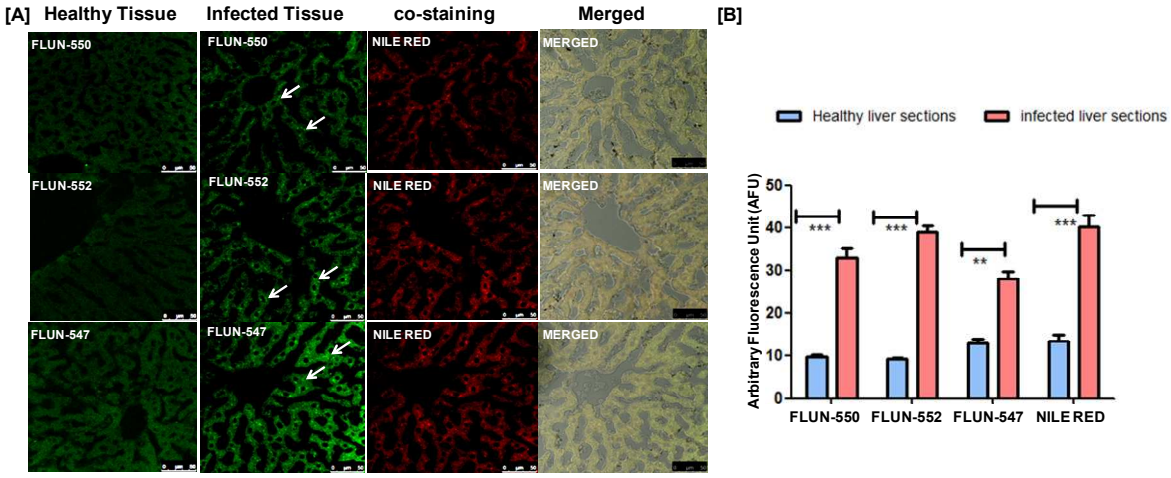

Figure 5. Confocal fluorescence image of healthy and infected liver sections [A] Dual staining with **FLUN-550, FLUN-552** and **FLUN-547** (100 nM) and Nile Red (300 nM) at 63X in *P. yoelii* MDR infected mouse. [B] Fluorescence signal quantification by LAS (Leica application suit). ***P 0.0004 (**FLUN-550**), <0.0001 (**FLUN-552**), 0.0009 (Nile Red) & **P =0.0016 (**FLUN-547**), statistical analysis by student t-test; Bar indicates 50µm.

To examine the staining pattern of lipids, **FLUN** derivatives (100 nM) were incubated in *P. yoelii* infected liver tissue sections for 5 minutes. Tissue sections were washed twice with PBS buffer and mounted with 75% glycerol for confocal imaging. A large number of clusters of lipid droplets were observed (Figure 5A, white arrows). Further the co-staining experiments with commercial LDs dye Nile Red showed similar staining pattern suggesting the selectivity of **FLUN**s for LDs in tissue sections. Based on the data obtained from the imaging of tissue sections on staining with different **FLUN** derivatives, the quantitative detection was done following standard protocol[10]. The results showed that **FLUN-550** and **FLUN-552** significantly increased the fluorescence intensity of the *Plasmodium yoelii* MDR infected specimen stained compared to healthy liver sections (Figure 5B and S9). The quantification analysis implicated three to four fold increased level of lipid accumulation in malaria infected liver tissues as compared to control.

LDs staining in human cancerous cervical tissue

We next examined the potential of the probes for lipid staining during cancer cell proliferation which requires the rapid synthesis of lipids for the generation of biological membranes. The accumulation of energy-rich lipids could provide cancer cells with energy during times of nutrient depletion. But the exact role of the deposition of lipid droplets in cancerous tissues is not clearly understood due to the lack of potential fluorescent probes, which could efficiently perform at tissue level. Therefore, the standardization of quick fluorescent labeling for these lipid droplets in cancerous as well as adjacent noncancerous tissues with these newly developed probes may help in better understanding of metabolic alterations during cell transformation and cancer development.

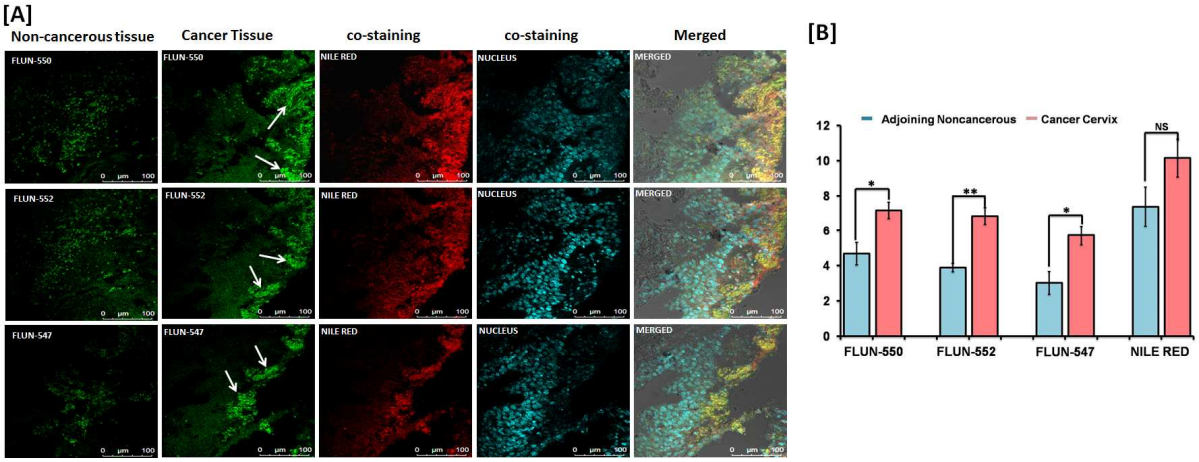

Figure 6. [A] Confocal fluorescence image of Cervical Cancer (IIIB Stage) vs. adjacent non-cancerous tissue sections. Co-staining of **FLUN-550**, **FLUN-552** and **FLUN-547** (200 nM) with Nile Red (200 nM) and To-Pro nuclear stain in serial section of cancer tissues; [B] Analyses of average fluorescence intensity of lipid droplets by **FLUN-550**, **FLUN-552** and **FLUN-547** assessed through Image J and Prism 3 software demonstrated a significant difference between cancerous and adjoining noncancerous cervix tissue sections. $*P < 0.05$, $**P = 0.0015$, Bar indicates 100 µm.

To check the potential application of the **FLUN** derivatives to stain lipid in tissue sections of cervical cancer, human cervical punch biopsies from cervical cancer patients were obtained from King George's Medical University, Lucknow, India in accordance with Institutional Ethics Committee and after patient's written consent (51 E.C.M. IIa/P1). The staining pattern of these novel probes by confocal fluorescence imaging was compared with Nile Red through

the co-staining experiments as shown in Figure 6. Staining of lipid droplets mostly co-localized in the cancerous tissue sections. The overall staining pattern was found to be quite different in the cancerous tissues as compared to the non-cancerous ones; as quite a few lipid accumulation pockets (lipid clusters) were observed in the cancerous sections (Figure 6A, white arrows) but not in the non-cancerous tissues (Figure 6A and S10). Moreover, we also quantified and compared overall lipid droplets in these stained sections through the measurement of fluorescence intensity using Image J software. This analysis established a significant difference in the lipid content of cancerous versus adjoining noncancerous tissues, using **FLUN** derivatives (Figure 6B). Statistical evaluation was performed through the student's t-test ($p < 0.05$) using Prism software. The quantitation analysis of fluorescence intensity of serial sections of cancer tissue stained by **FLUN-550** and **FLUN-552** revealed a significant increase in the lipid content of cancerous tissues as compared to the adjoining non-cancerous counterpart. Similarly in the case of Nile red staining, the fluorescence intensities of lipid droplets between cancerous and adjoining non-cancerous tissue sections was also enhanced but the intensity was statistically non-significant possibly due to low LDs selectivity by Nile Red.[17-19] As per tissue analysis after 6 days, these new probes were found to be more stable as compare to nile red staining. To the best of our knowledge, this is the first report of yellow fluorescent probes for simple, selective and quantitative detection of lipid droplets in cancerous and non-cancerous tissue sections of the third stage of human cervical cancer patients.

▪ CONCLUSION

In conclusion, we have developed new fluoranthene based yellow fluorescent probes **FLUN-550** and **FLUN-552** for selective staining of lipid droplets in live 3T3-L1 pre-adipocytes and live *L. donovani* promastigotes. We have designed new probes by conjugating ethanolamine moiety so as to mimic the head groups of phospholipids present in biological membrane for

hydrophobic-hydrophobic interactions. These new probes showed visible excitability, aqueous compatibility, high stokes shift (210-230 nm), good quantum yield and photostability. The confocal fluorescence imaging and quantitative detection of lipid droplets in liver sections of Plasmodium yoelii infected mouse and human cervical cancerous tissues revealed significantly increased accumulation of lipids as compared to control. Such quantitative detection studies are difficult to achieve and have not been reported in these different tissues prior to this study. Considering these encouraging results, new yellow fluorescent probes (**FLUN-550** and **FLUN-552**) are useful for early diagnosis of cervical cancer patients. According to the present study, **FLUN-550** and **FLUN-552** observed to be really significant and more stable as compare to commercially available stain Nile Red. These new findings will not only be beneficial for diagnosis but also for understanding the excess accumulation of lipids during pathogenesis of malaria, cancer and metabolic disorders. Further studies with these probes for significant quantitative analysis of lipid droplets can be established as a novel cancer biomarker in different grades of cancer patient biopsy samples.

▪ EXPERIMENTAL SECTION

General Information.

The chemicals and solvents of analytical grade were used without further purification. Synthetic details of the fluorescent probes have been given in Scheme 1 and the supporting information.

^{1}H NMR spectra were recorded at 400 and 300 MHz and ^{13}C NMR spectra were recorded at 100 MHz. Chemical shifts are reported in parts per million shift (δ-value) from Me_4Si (δ 0 ppm for ^{1}H) or based on the middle peak of the solvent ($CDCl_3$) (δ 7.26 ppm for ^{1}H NMR and δ 77.00 ppm for ^{13}C NMR) or DMSO-d_6 (δ 2.50 ppm for ^{1}H NMR and δ 40.00 ppm for ^{13}C NMR) as an internal standard. Signal pattern are indicated as s, singlet; d, doublet; t,

triplet; m, multiplet. Coupling constant (*J*) is given in Hertz. Infrared (IR) spectra were recorded in KBr disc and reported in wave number (cm^{-1}). The ESI-MS were recorded on MICROMASS Quadro-II LCMS system. The HRMS spectra were recorded as ESI-HRMS on a mass analyzer system. All the reactions were monitored by TLC and visualization was done with UV light (254 nm). Agilent Cary 100 UV-Vis spectrophotometer was used for absorbance measurements. A Varian Cary Eclipse spectrofluorophotometer was used for fluorescence measurements. For cell imaging, confocal laser scanning microscope (Lieca, Germany) was used. Further, fluorescence intensity was quantified using image J software (Image J, National Institute of Health, Bethesda, MD). Fluorescence signal quantification was done by LAS (Leica application suit) and Prism 3 software.

Cell culture and Staining studies (3T3-L1 pre-adipocytes and *L. donovani*)

Cell Culture: 3T3-L1 pre-adipocytes were cultured in DMEM with 10% heat-inactivated FBS at 37 °C. After reaching 70% confluence, cells were seeded for two days before starting experiments. *Leishmania donovani* (strain MHOM/IN/80/Dd8) promastigotes were cultured as described previously. Briefly, cells were cultured in Dulbecco's Modified Eagles Medium (DMEM) with phenol red, L-glutamine and 4.8g/L D-glucose supplemented with 10% heat inactivated FBS and sodium pyruvate. Cell were checked for their health periodically and maintained in standard tissue culture flasks. After reaching an approximate density of 10^6 cells/ml they were prepared for incubation.

Confocal Microscopy: 3T3-L1 pre-adipocytes adhered to confocal microscopy dishes were incubated with the dye (**FLUN-552** and **FLUN-547**) in DMEM for 30 min at 37°C. They were washed and stained with 1 μM Hoechst 33342 (Invitrogen) for 10 min. Samples were analyzed under a laser scanning microscope LSM 510 META (Carl Zeiss, Jena, Germany).

Images were acquired with a 63X Plan Apochromat Oil Phase II 1.4 objective. Lasers used were Diode 405 nm, Ar/ML 458/477/488/514 nm and DPSS 561nm.

L. donovani cells, briefly after harvesting, were incubated with 100 nM of dye **FLUN-552** and **FLUN-547** in medium for 2 hrs. at room temperature (DMSO in the media was merely 0.01% v/v). Afterwards, they were washed with PBS. Cells were then adhered to poly-L-lysine coated cover slips and immediately processed for confocal imaging. Stacks of images at different focal planes were acquired and merged to create a movie with AIM 4.0 software.

Analysis: Images were analyzed with the LSM Image Examiner software (Carl Zeiss). The 2.5D option was used to display the fluorescence peaks of fluorescent LDs, which are distinct from the background (i.e. fluorescent against non-fluorescent background). This mode displays two-dimensional fluorescence intensity information in a pseudo-3D image. The increase in fluorescence intensity is color coded as change in color was observed from blue to red. The viewing angle was set at 45º at all times. Rotation at both axes was set to 0º; filled option with rainbow palette was used.

Dual staining with Nile Red: Cells (*L. donovani*), briefly after harvesting, were incubated with 100 nM **FLUN-552** and **FLUN-547** for 2 hrs. Afterwards, they were washed with PBS and further incubated with 300 nM Nile Red upto 10 minutes and washed again with PBS. Cells were then immediately adhered to poly-L-lysine coated coverslips and processed for microscopic examination. The images were analyzed using with the LSM Image Examiner software (Zeiss). Nile red staining showed fluorescence with excitation wavelength at 561 nm and emission at 575 nm long pass whilst excitation wavelength of Fluorescence Probes was 405 nm and emission at band of 505 nm-570 nm.

Tissue preparation and staining studies (Healthy and Infected Liver Tissue)

Tissue preparation: To evaluate fat deposition, liver specimen from healthy mice and *P. yoelii* MDR infected mice (at 50% parasitaemia) were embedded using tissue OCT-freeze medium and sliced into 10 µm-thick sections using a cryostat microtome (LEICA).

Nile Red staining: A stock solution of Nile red (10 mM) in acetone was prepared and stored chilled and protected from light. A fresh staining solution of Nile red (300 nM) was made by diluting the stock in 75% glycerol followed by brisk vortexing. The glycerol-dye solution was then briefly degassed by vacuum to remove bubbles. To stain frozen sections of liver, a drop of glycerol staining solution was added to each section and incubated for 5 min. After incubation, the sections were examined by confocal microscopy.[27]

Fluorescent probes (**FLUN-550**, **FLUN-552** and **FLUN-547**) staining: A stock solution of each probe (10 mM) namely **FLUN-550**, **FLUN-552** and **FLUN-547** in PBS buffer (DMSO in the media was merely 0.01% v/v) was prepared and stored, chilled and protected from light. A fresh staining solution of probe (100 nM) was made by diluting the stock in PBS buffer. To stain frozen section of liver, a drop of probe was added to each section, incubated for 5 min. After washing two times with PBS buffer, tissue sections were mounted with 75% glycerol and examined.

Dual Staining with Nile Red and Probes: Frozen liver sections were incubated for 5 min with Nile red and probe, washed two times with PBS and mounted with 75% glycerol.

Confocal microscopy: The sections were examined with Leica SP8 confocal microscope at 63X with immersion oil. Excitation wavelength of Fluorescence Probes was 405 nm and

emission at band of 505 nm-570 nm and Nile red staining showed fluorescence in red channel.

Tissue preparation and staining studies (Cancerous Cervical Tissue)

Tissue sections of cancer samples: Human cervical punch biopsies from cervical cancer patients were obtained from King George's Medical University, Lucknow, India in accordance with institutional Ethics Committee and after patient's written consent (51 E.C.M. IIa/P1). Tissues were immediately fixed in 4% neutral buffered formalin and then embedded into paraffin wax to make the blocks of these tissues. Now 5 µm serial sections were cut from these tissue blocks and placed on polylysine coated glass slides. These slides were stored at room temperature for further experiments.

Fluorescent probes (FLUN-550, FLUN-552 and 547) co-staining with Nile Red: Stock (5mM) solutions of probe **FLUN-550** and its derivatives (**FLUN-552** and **FLUN-547**) were prepared in analytical grade DMSO (DMSO in the media was merely 0.01% v/v); whereas stock solution of Nile Red (5mM) was prepared in acetone. All the stocks were stored chilled and protected from light. Fresh dilutions (200 nM) of **FLUN-550** and Nile Red were made in sterile PBS buffer. Now the slides of the tissue sections were heated at 60°C for 20 min, deparaffinized with xylene and rehydrated with various grades of ethanol. Then, these tissue sections were incubated with **FLUN** derivatives or Nile Red (200 nM) for 15 minutes and washed twice with PBS buffer. The sections were then incubated with the nuclear stain To-Pro (1 µM) for 20 minutes and washed twice with PBS buffer. Stained slides were mounted with a glass cover slip using 75% glycerol.

▪ ACKNOWLEDGMENTS

AG thanks Department of Atomic Energy (DAE-SRC) for Outstanding Investigator Award (21/13/2015-BRNS/35029). Authors thank CSIR, New Delhi for research fellowships. We

acknowledge Mrs. Rima A. Sarkar for confocal imaging of tissue sections and SAIF-CDRI for providing spectral data. The CDRI communication number is 9674.

■ ASSOCIATED CONTENT

Supporting Information

Spectroscopic data, ^{1}H, ^{13}C NMR and UV-FL spectra of all the compounds are given in supporting. This material is available free of charge via the internet at http://pubs.acs.org

■ REFERENCES

[1] Martin, S., and Parton, R. G. (2006) Lipid droplets: a unified view of a dynamic organelle. *Nat. Rev. Mol. Cell Biol*. *7,* 373-378.

[2] Zhang, H., Wang, Y., Li, J., Yu, J., Pu, J., Li, L., Zhang, H., Zhang, S., Peng, G., Yang, F. and Liu, P. (2011) Proteome of Skeletal Muscle Lipid Droplet Reveals Association with Mitochondria and Apolipoprotein A-I. *J. Proteome Res. 10*, 4757-4768.

[3] Boulant, S. P., Adams, T. and McLauchlan, J. (2007) Disrupting the association of hepatitis C virus core protein with lipid droplets correlates with a loss in production of infectious virus. *J. Gen. Virol., 88*, 2204-2213.

[4] Miyanari, Y., Atsuzawa, K., Usuda, N., Watashi, K., Hishiki, T., Zayas, M., Bartenschlager, R., Wakita, T., Hijikata, M. and Shimotohno, K. (2007) The lipid droplet is an important organelle for hepatitis C virus production. *Nat. Cell Biol.*, *9*, 1089-1097.

[5] Davis, J., Crunk, A. E., Monks, J., Murakami, A., Jackman, M., MacLean, P. S., Ladinsky, M., Bales, E., Cain, S., Orlicky, S. D. J. and McManaman, J. L. (2013) Dynamic regulation of hepatic lipid droplet properties by diet. *PLoS One*, *8* e67631.

[6] Yonezawa, T., Kurata, R., Kimura, M. and Inoko, H. (2011) Which CIDE are you on? Apoptosis and energy metabolism. Mol. *BioSyst.*, *7*, 91-100.

[7] Medes, G., Thomas, A. and Weinhouse, S. (1953) Metabolism of neoplastic tissue. IV. A study of lipid synthesis in neoplastic tissue slices in vitro. *Cancer research*, *13*, 27-29.

[8] Baenke, F., Peck, B. and Miess, H. (2013) A. Schulze, Hooked on fat: the role of lipid synthesis in cancer metabolism and tumour development. *Disease Models and Mechanisms*, *6*, 1353-1363.

[9] Ohsaki, Y., Suzuki, M. and Fujimoto, T. (2014) Open Questions in Lipid Droplet Biology. *Chem. Biol. 21,* 86-96.

[10] Mehlem, A., Hagberg, C. E., Muhl, L. and Eriksson, U. (2013) A. Falkevall, Imaging of neutral lipids by oil red O for analyzing the metabolic status in health and disease. *Nat Protoc.*, *8*, 1149-1154.

[11] Fowler, S. D. and Greenspan, P. (1985) Application of Nile red, a fluorescent hydrophobic probe, for the detection of neutral lipid deposits in tissue sections: comparison with oil red O. *J. Histochem. Cytochem., 33*, 833-836.

[12] Bonilla, E. and Prelle, A. (1987) Application of nile blue and nile red, two fluorescent probes, for detection of lipid droplets in human skeletal muscle. *J. Histochem. Cytochem.*, *35*, 619–621.

[13] De Bock, K., Dresselaers, T., Kiens, B., Richter, E. A., Van Hecke, P. and Hespel, P. (2007) Evaluation of intramyocellular lipid breakdown during exercise by biochemical assay, NMR spectroscopy, and Oil Red O staining. *Am. J. Physiol., 293*, E428-E434.

[14] Shaw, C. S., Jones, D. A. and Wagenmakers, A. J. M. (2008) Network distribution of mitochondria and lipid droplets in human muscle fibres. *Histochem. Cell. Biol.*, *129* 65-72.

[15] Shaw, C. S., Sherlock, M., Stewart, P. M. and Wagenmakers, A. J. M. (2009) Adipophilin distribution and colocalization with lipid droplets in skeletal muscle. *Histochem. Cell Biol.*, *131*, 575-581.

[16] Zietkowski, D., deSouza, N. M., Davidson, R. L. and Payne, G. S. (2013) Characterisation of mobile lipid resonances in tissue biopsies from patients with cervical cancer and correlation with cytoplasmic lipid droplets. *NMR Biomed. 26*, 1096-1102.

[17] Listenberger,L. L. and Brown, D. A. (2007) *Fluorescent detection of lipid droplets and associated proteins. Current Protocols in Cell Biology*, Wiley & Sons, Inc., chapter 24, unit 24.2.1.

[18] Cosgrave, L., Devocelle, M., Forster, R. J. and Keyes, T. E. (2010) Multimodal cell imaging by ruthenium polypyridyl labelled cell penetrating peptides. *Chem. Commun. 46,* 103.

[19] Rumin, J., Bonnefond, H., Saint-Jean, B., Rouxel, C., Sciandra, A., Bernard, O., Cadoret, J.-P. and Bougaran, G. (2015) The use of fluorescent Nile red and BODIPY for lipid measurement in microalgae. *Biotechnol. Biofuels*, 8, 42.

[20] Spandl, J., White, D. J., Peychl, J. and Thiele, C. (2009) Live cell multicolor imaging of lipid droplets with a new dye, LD540. *Traffic*, *10*, 1579–1584.

[21] Neef, A. B. and Schultz, C. (2009) Selective Fluorescence Labeling of Lipids in Living Cells. *Angew. Chem., Int. Ed.*, *48,* 1498–1500.

[22] Lee,Y., Na, S., Lee, S., Jeon, N. L. and Park, S. B. (2013) Optimization of Seoul-Fluor-based lipid droplet bioprobes and their application in microalgae for bio-fuel study. *Mol. BioSyst., 9*, 952-956.

[23] Lee, J. H., So, J. H., Jeon, J. H., Choi, E. B., Lee, Y. R., Chang, Y. T., Kim, C. H., Bae, M. A. and Ahn, J. H. (2011) Synthesis of a new fluorescent small molecule probe and its use for *in vivo* lipid imaging. *Chem. Commun.*,*47*, 7500–7502.

[24] Goel, A., Sharma, A., Kathuria, M., Bhattacharjee, A., Verma, A., Mishra, P. R., Nazir, A. and K. Mitra, (2014) New Fluoranthene FLUN-550 as a Fluorescent Probe for Selective Staining and Quantification of Intracellular Lipid Droplets. *Org. Lett.,16*, 756−759.

[25] Sk, B., Thakre, P. K., Tomar, R. S. and Patra, A. (2017) A Pyridoindole-Based Multifunctional Bioprobe: pH-Induced Fluorescence Switching and Specific Targeting of Lipid Droplets *Chem. – Asian J.*, *12*, 2501-2509.

[26] Wu, A., Kolanowski, J. L., Boumelhem, B. B., Yang, K., Lee, R., Kaur, A., Fraser, S. T., New, E. J.and Rendina, L. M. (2017) A Carborane-Containing Fluorophore as a Stain of Cellular Lipid Droplets *Chem. Asian J.*, *12*, 1704-1708.

[27] Daemen, S., van Zandvoort, M. A., Parekh, S. H. and Hesselink, M. K. (2016) Microscopy Tools for the Investigation of Intracellular Lipid Storage and Dynamics. *Mol. Metabol., 5*, 153-163.

[28] Wang, Z., Gui, C., Zhao, E., Wang, J., Li, X., Qin, A., Zhao, Z., Yu, Z. and Tang, B. Z. (2016) Specific Fluorescence Probes for Lipid Droplets Based on Simple AIEgens. *ACS Appl. Mater. Interfaces 8*, 10193−10200.

[29] Sharma, A., Umar, S., Kar, P., Singh, K., Sachdev, M. and Goel, A. (2016) A new type of biocompatible fluorescent probe AFN for fixed and live cell imaging of intracellular lipid droplets. *Analyst*, *141,* 137-143.

[30] Jiang, M., Gu, X., Lam, J. W. Y., Zhang, Y., Kwok, R. T. K., Wong, K. S. and Tang, B. Z. (2017) Two-photon AIE bio-probe with large Stokes shift for specific imaging of lipid droplets. *Chem. Sci.*, *8*, 5440-5446.

[31] Appelqvist, H, Stranius, K., Boerjesson, K., Nilsson, K. P. R. and Dyrager, C. (2017) Benzothiadiazole Derivatives as Fluorescence Imaging Probes: Beyond Classical Scaffolds. *Bioconjugate Chem.*, *28*, 1363-1370.

[32] Kang, M., Gu, X., Kwok, R. T., Leung, C. W., Lam, J. W., Li, F. and Tang, B. Z. (2016) A near-infrared AIEgen for specific imaging of lipid droplets. *Chem. Commun.*, *52*, 5957-5960

[33] Lee, B., Park, B. G., Cho, W., Lee, H. Y., Olasz, A., Chen, C.-H., Park, S. B. And Lee, D. (2016) BOIMPY: Fluorescent Boron Complexes with Tunable and Environment-Responsive Light-Emitting Properties *Chem. Eur. J.*, *22*, 17321 -17328

[34] Guo, L., Tian, M., Feng, R., Zhang, G., Zhang, R., Li, X., Liu, Z., He, X., and Sun, J. Z. and Yu, X. (2018) Interface-Targeting Strategy Enables Two-Photon Fluorescent Lipid Droplet Probes for High-Fidelity Imaging of Turbid Tissues and Detecting Fatty Liver, *ACS Appl. Mater. Interfaces 10*, 10706-10717.

[35] Mota, A. A. R., Correa, J. R., de Andrade, L. P., Assumpção, J. A. F., de Souza Cintra, G. A., Junior, L.H. F- W., da Silva, de Oliveira, A. H. C. B. and Neto, B. A. D. (2018) From Live Cells to Caenorhabditis elegans: Selective Staining and Quantification of Lipid Structures Using a Fluorescent Hybrid Benzothiadiazole Derivative *ACS Omega 3*, 3874-3881.

[36] Collot, M., Fam, T. K., Ashokkumar, P., Faklaris, O., Galli, T., Danglot, L. and Klymchenko, A. S. (2018) Ultrabright and Fluorogenic Probes for Multicolor Imaging and Tracking of Lipid Droplets in Cells and Tissues *J. Am. Chem. Soc.140*, 5401-5411

[37] Goel, A., Sharma, A., Mitra, K., Bhattacharjee, A. and Kathuria, M. Substituted fluoranthene-7-carbonitriles/esters as fluorescent dyes for cell imaging applications, CSIR Pat. No.: 807DEL2013 dated 19-Mar-2013; PCT/IN2014/000156 dated 10-Mar-2014.

[38] Goel, A., Parihar, A., Mishra, P., Varshney, S., Nag, P., Beg, M., Gaikwad, A. and Rath, S. K. (2013) Design and synthesis of novel pyranone-based insulin sensitizers exhibiting *in vivo* hepatoprotective activity. *Med. Chem. Commun*., *4*, 1532-1536.

[39] Rakotomanga, M., Blanc, S., Gaudin, K., Chaminade, P. and Loiseau, P. M. (2007) Miltefosine affects lipid metabolism in Leishmania donovani promastigotes. *Antimicrob. Agents Chemother*., *51,* 1425-1430.

[40] Croft, S. L. and Yardley, V. (2002) Chemotherapy of leishmaniasis. *Curr. Pharm. Des*. *8*, 319-342.

[41] Croft, S. L. and Coombs, G. H. (2003) Leishmaniasis– current chemotherapy and recent advances in the search for novel drugs. *Trends Parasitol*., *19*, 502-508.

[42] Bajpai, R. and Dutta, G. P. (1990) Role of fatty infiltration in pathology of malaria. *Life Sci.*, *47*, 25-28.

[43] Siddiqi, N. J., Puri, S. K., Dutta, G. P., Maheshwari, R. K. and Pandey, V. C. (1999) Studies on hepatic oxidative stress and antioxidant defence system during chloroquine/poly ICLC treatment of Plasmodium yoelii nigeriensis infected mice. *Mol. Cell. Biochem.*, *194*, 179-183.

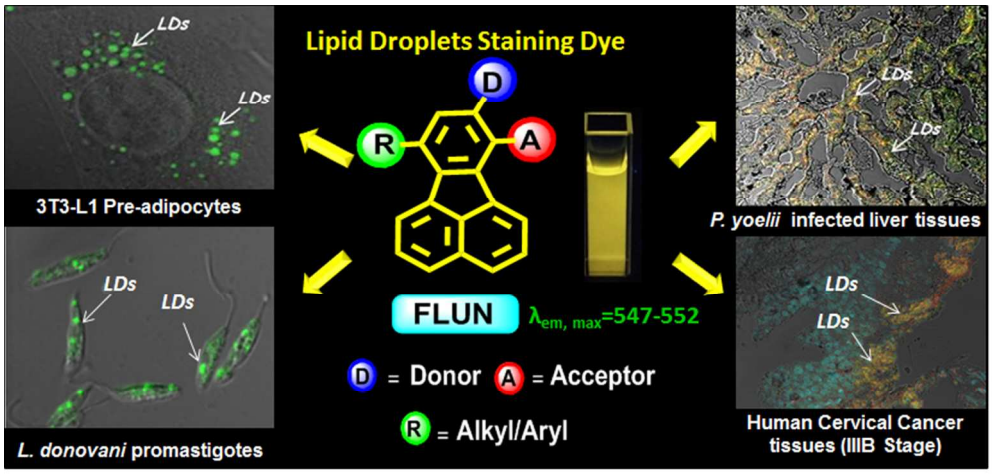

TOC Graphics

70x33mm (300 x 300 DPI)